Received: 7 July 2022 | Revised: 27 August 2022 | Accepted: 15 September 2022

DOI: 10.1002/bte2.20220024

RESEARCH ARTICLE

BATTERY ENERGY Open Access

WILEY

Enhanced Li-ion conductivity of $Li_7La_3Zr_2O_{12}$ by simultaneous substitution of aluminum and niobium using a modified sol–gel method

Jin Won Kim[1,2,3] | **James L. Digol**[1] | **Sungyool Bong**[1,2,3] | **Jaeyoung Lee**[1,2,3]

[1]School of Earth Sciences and Environmental Engineering, Gwangju Institute of Science and Technology (GIST), Gwangju, Republic of Korea

[2]ErtlCenter for Electrochemical and Catalysis, Gwangju Institute of Science and Technology (GIST), Gwangju, Republic of Korea

[3]International Future Research Center of Chemical Energy Storage and Conversion Processes, Gwangju Institute of Science and Technology (GIST), Gwangju, Republic of Korea

Correspondence
Jaeyoung Lee, School of Earth Sciences and Environmental Engineering, Gwangju Institute of Science and Technology (GIST), Gwangju, Republic of Korea.
Email: jaeyoung@gist.ac.kr

Funding information
NRF Korea, Grant/Award Number: 2021K1A48A01079455

Abstract

By increasing technical demand for long-lasting and safer batteries against thermal explosion, garnet-type cubic phase $Li_7La_3Zr_2O_{12}$ (LLZO) is a promising solid electrolyte as a next-generation advanced battery. In this work, we studied Al and Nb co-doped $Li_{6.25-y}Al_{0.25}La_3Zr_{2-y}Nb_yO_{12}$ ($0 \leq y \leq 0.30$) electrolytes prepared using a modified sol–gel method. X-ray diffraction and electrochemical analyses probed the synergistic effect of Al and Nb simultaneous substitution on the microstructure and ionic conductivity. In conclusion, an optimal amount of Al and Nb enhances densification and ionic conductivity, and then $Li_6Al_{0.25}La_3Zr_{1.75}Nb_{0.25}O_{12}$ achieves the highest relative density of 94% and total ionic conductivity of $5.41 \times 10^4\ S\ cm^{-1}$ at 30°C.

KEYWORDS
LLZO, simultaneous substitution, sol–gel synthesis, solid electrolyte

1 | INTRODUCTION

Lithium-ion batteries (LIBs) are considered the most promising energy storage materials for various applications such as wearable electronic devices, gadgets, and electric vehicles because of their high volumetric energy density, long cycle lifetime, and fast charge–discharge rates.[1,2] However, safety issues arising from thermal explosion, mainly caused by the flammability of organic liquid electrolytes, have impeded practical utilization, especially for electric vehicles. Thus, development of new electrolytes is necessary to replace conventional organic liquid electrolytes. As a better alternative, inorganic solid electrolytes eliminate this safety concern and are considered ideal candidates for next-generation solid-state lithium-based batteries.

Among the three kinds of solid electrolytes such as polymers, sulfide, and oxide-based electrolytes, cubic phase $Li_7La_3Zr_2O_{12}$ (LLZO) has received considerable attention due to its comparable ionic conductivity to that of liquid electrolytes, low activation energy, excellent thermal performance, high Li^+ ion transport number, and acceptable elastic property.[3–5] Although oxide-based solid electrolytes have interface instability issues with Li metal, they have been considered promising options for all-solid-state lithium metal-based batteries in mass production. This is because of their less susceptibility to decomposition resulting from the oxygen and humidity in the air compared to sulfide-based solid electrolytes. To stabilize the cubic structure of LLZO, doping with aliovalent elements has been performed by substituting the sites for Li (Al, Fe, Ga), La (Sr, Y, Ce), and/or Zr (Nb, Ta, Sb, Mg, Sc, Zn, Ru, W, Te).[6–8] Among these dopants, Al has been intensively studied and found to either (i) stabilize the cubic structure by its substitution at the lithium sites (increased Li vacancy) or (ii) yield a denser material by acting as a sintering aid. This is critical because structural stability and bulk density directly affect the ionic conductivity of LLZO electrolytes.[9]

Based on this, codoping of multiatom is considered to be a new model for further tailoring ionic conductivity and elucidating the structure–property correlation. Codoping of LLZO with Al and other cations such as Si, Te, and Ga significantly affects the microstructure and crystal structure.[10–13] Among many alternatives, in this work, we focus on substituting the Zr site with Nb to stabilize the cubic phase LLZO.

As the primary purpose of use of solid electrolytes is to enhance ionic conductivity, the synthetic procedure is also one of the crucial factors. This is because minimizing grain boundaries and impurity phases facilitates low ionic resistance. In this respect, the sol–gel method is powerful in reducing grain boundaries. In the case of the LLZO pellets synthesized by the sol–gel method, only the bulk contributes to the lithium-ion conduction as the crystallite size, while use of the conventional pellet method prepared by solid-state synthesis yields polycrystalline behavior with grain boundaries and bulk with a much smaller crystallite size.[14–16]

In this paper, we report the properties of the LLZO-based garnet electrolyte $Li_{6.25\text{-}y}Al_{0.25}La_3Zr_{2-y}Nb_yO_{12}$ ($0 \leq y \leq 0.30$) prepared by the simultaneous substitution of Al and Nb using a modified sol–gel method. We observed that the Al and Nb codoped LLZO electrolyte prepared using the sol–gel method benefited from the combined influence on the garnet's crystalline structure and lithium-ion conductance as a function of the relative densification of the pellets.

2 | EXPERIMENTAL SECTION

2.1 | Synthesis of a $Li_{6.75}Al_{0.25}La_3Zr_{2-y}Nb_yO_{12}$ garnet electrolyte

(All bulk $Li_{6.75}Al_{0.25}La_3Zr_{2-y}Nb_yO_{12}$ $y = 0-0.30$) powders used in this work were synthesized using a modified sol–gel method.[16] $LiNO_3$ anhydrous (99%; Sigma-Aldrich) was used as a Li source, and $La(NO_3)_3{\cdot}6H_2O$ (99.9%; Sigma-Aldrich) and $ZrO(NO_3)_2{\cdot}xH_2O$ (99%; Sigma-Aldrich, $x \approx 2$, measured by thermal gravimetric analysis) were used as precursors of La and Zr. Citric acid (99%; Sigma-Aldrich) and ethylene glycol (99%; Sigma-Aldrich) were used as a complexing agent and a surfactant, respectively. To prepare the samples with Al and Nb codoping, $Al(NO_3)_3{\cdot}9H_2O$ (98%; Sigma-Aldrich) and $NbCl_2$ (99.9%; Sigma-Aldrich) were used as Al and Nb sources, respectively.

The Al and Nb codoped LLZO synthetic processes using the modified sol–gel method were categorized into three steps: gelation, calcination, and the final sintering process after pelletizing the powder. First, for the gelation step, 10% excess of $LiNO_3$ and stoichiometric amounts of powdery precursors were put into a solvent mixture of citric acid with ethylene glycol. The stoichiometric atom ratio of Li and Al was fixed to 6.75:0.25 in this work following our previous study. The Al and Nb codoped LLZO synthetic processes using the modified sol–gel method were categorized into three steps: gelation, calcination, and the final sintering process after pelletizing the powder. First, for the gelation step, 10% excess of $LiNO_3$ and stoichiometric amounts of powdery precursors were put into a solvent mixture of citric acid with ethylene glycol. The stoichiometric atom ratio of Li and Al was fixed to 6.75:0.25 in this work following our previous study.[17] The only stoichiometric Zr and Nb atom ratios were controlled in various ranges of $2-y{:}y$ ($0 \leq y \leq 0.30$) to investigate the effects of Nb doping on the properties of an Al-doped LLZO solid electrolyte. For the calcination step, after the dark brownish gel resultant was formed at 80°C, the brown resin powders as a starting powder were obtained through an evaporation step at 250°C over 4 h. The pulverized starting powders were transferred to an alumina crucible and then calcined at 400°C, 600°C, or 900°C for 10 h under an air atmosphere. As a final sintering process, the as-calcined powders were pelletized under isostatic pressure (100 MPa) and sintered at 1200°C for 7 h, while the pellet samples were covered with the same mother powder to avoid lithium loss. All the pellet samples that we used in this paper were circular with a 1.8 cm diameter and were 500 μm in thickness. The only stoichiometric Zr and Nb atom ratios were controlled in various ranges of $2-y{:}y$ ($0 \leq y \leq 0.30$) to investigate the effects of Nb doping on the properties of an Al-doped LLZO solid electrolyte. For the calcination step, after the dark brownish gel resultant was formed at 80°C, the brown resin powders as a starting powder were obtained through an evaporation step at 250°C over 4 h. The pulverized starting powders were transferred to an alumina crucible and then calcined at 400°C, 600°C, or 900°C for 10 h under an air atmosphere. As a final sintering process, the as-calcined powders were pelletized under isostatic pressure (100 MPa) and sintered at 1200°C for 7 h, while the pellet

samples were covered with the same mother powder to avoid lithium loss. All the pellet samples that we used in this paper were circular with a 1.8 cm diameter and were 500 μm in thickness.

2.2 | Physicochemical and electrochemical characterization

The relative density (RD) and the relative shrinkage (RS) of the pellet samples before and after the sintering process were calculated using the Archimedes method as follows[18]:

$$\mathrm{RD}(\%) = (\rho/\rho_{\mathrm{theoretical}}) \times 100 \ \ (\rho_{\mathrm{theoretical}} \approx 5.107\ \mathrm{g\ cm^{-3}}), \tag{1}$$

$$\mathrm{RS}(\%) = [(d_0 - d)/d_0] \times 100, \tag{2}$$

where ρ and $\rho_{\mathrm{theoretical}}$ are the bulk density and the theoretical density, respectively, and d_0 and d are the diameters of pressed and sintered pellets, respectively.

X-ray diffraction (XRD) analysis (X'Pert PRO Multi-Purpose X-ray Diffractor, PANalytical) with Cu Kα1 radiation was used to monitor the phase formation of all powders, and Rietveld refinement analysis was carried out using HighScore Plus software to quantify structural parameters. The cross-sectional microstructure of the pellet samples was measured using a field-emission scanning electron microscope (FE-SEM S-4700; Hitachi).

For the Li-ion conductivity measurement, thin Au films were sputtered on the top and bottom sides of the pellets to act as ionically blocking layers. The Au-sputtered LLZO pellets were measured using a Teflon-lined Swagelok cell at various temperatures. AC impedance measurements (Zennium Electrochemical Workstation) were performed using an impedance analyzer measuring over the frequency range of 4 mHz–100 mHz with a 50 mV amplitude.

3 | RESULTS AND DISCUSSION

The ionic conductivity of Li garnet-type LLZO electrolytes strongly relies on crystallographic structures. The general LLZO structure has been reported for two polymorphs of a tetragonal structure ($I4_1$/acd) and a cubic structure (Ia-3d). The main structural difference between the two phases is the Li-ion occupancy in each crystallographic site, in which Li ions are partially occupied in the cubic phase but are fully occupied in

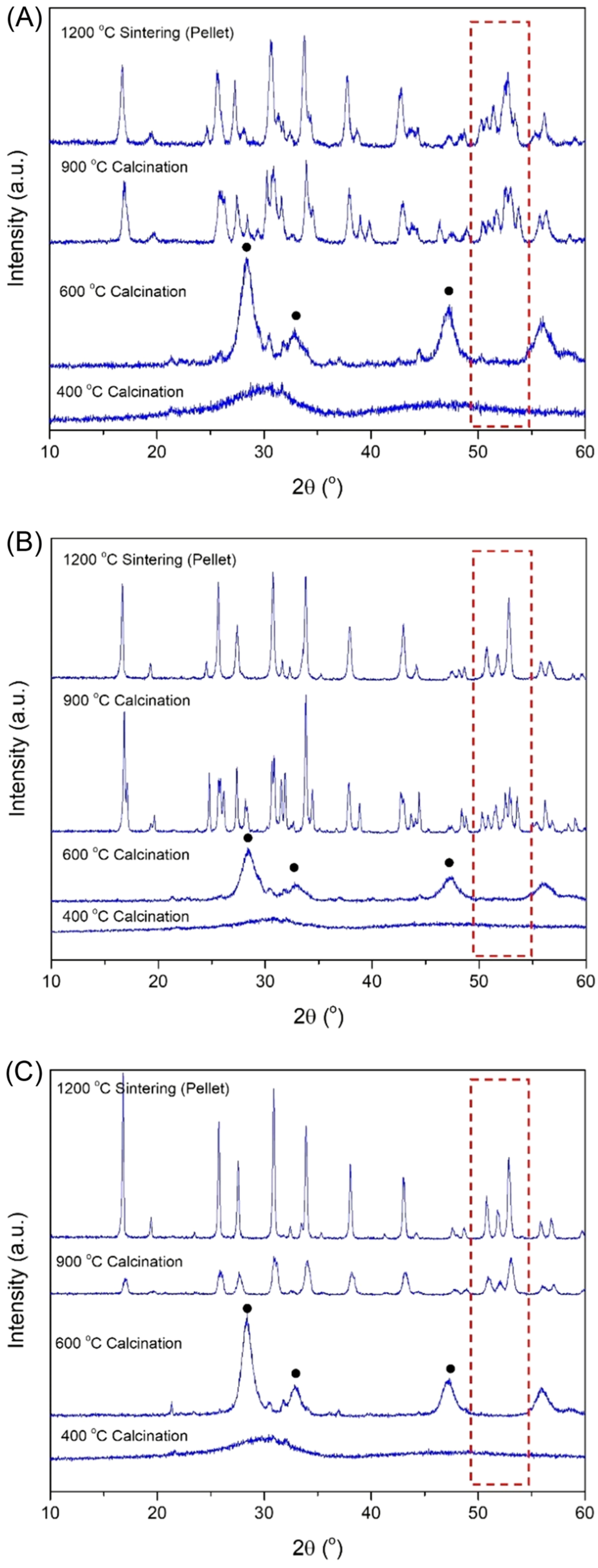

FIGURE 1 Changes of XRD patterns of three samples: (A) bare LLZO, (B) Al single-doped LLZO, and (C) Al and Nb dual-doped LLZO at different calcination and sintering temperatures (400°C, 600°C, 900°C, and 1200°C). A black closed circles indicate the pyrochlore ($La_2Zr_2O_7$) impurity phase. LLZO, $Li_7La_3Zr_2O_{12}$; XRD, X-ray diffraction.

the tetragonal phase.[19] The phase transition from tetragonal to cubic structures occurs following an increase of the calcination temperature and the hetero-atom dopant effect. Figure 1 shows the transition of the tetragonal phase into the cubic phase at various sintering temperatures and with the addition of hetero-atom dual dopants (Al and Nb). For the calcination step at three different temperatures, amorphous structures and impurities like the pyrochlore phase only appeared at 400°C and 600°C in all samples, whereas LLZO crystalline structures were formed during the 900°C calcination step. The XRD patterns of the cubic (ICSD 98-026-1302) and tetragonal (ICSD 01-078-6708) phases could be recognized by three peaks in the cubic phase and multi peaks in the tetragonal phase in the range of 50–55°. As shown in Figure 1A, it was shown that a high sintering temperature over 1200°C didn't change the tetragonal phase into the cubic phase without any hetero-atom doping step. Unlike bare LLZO samples as a reference, the cubic phase appeared in Al single-doped

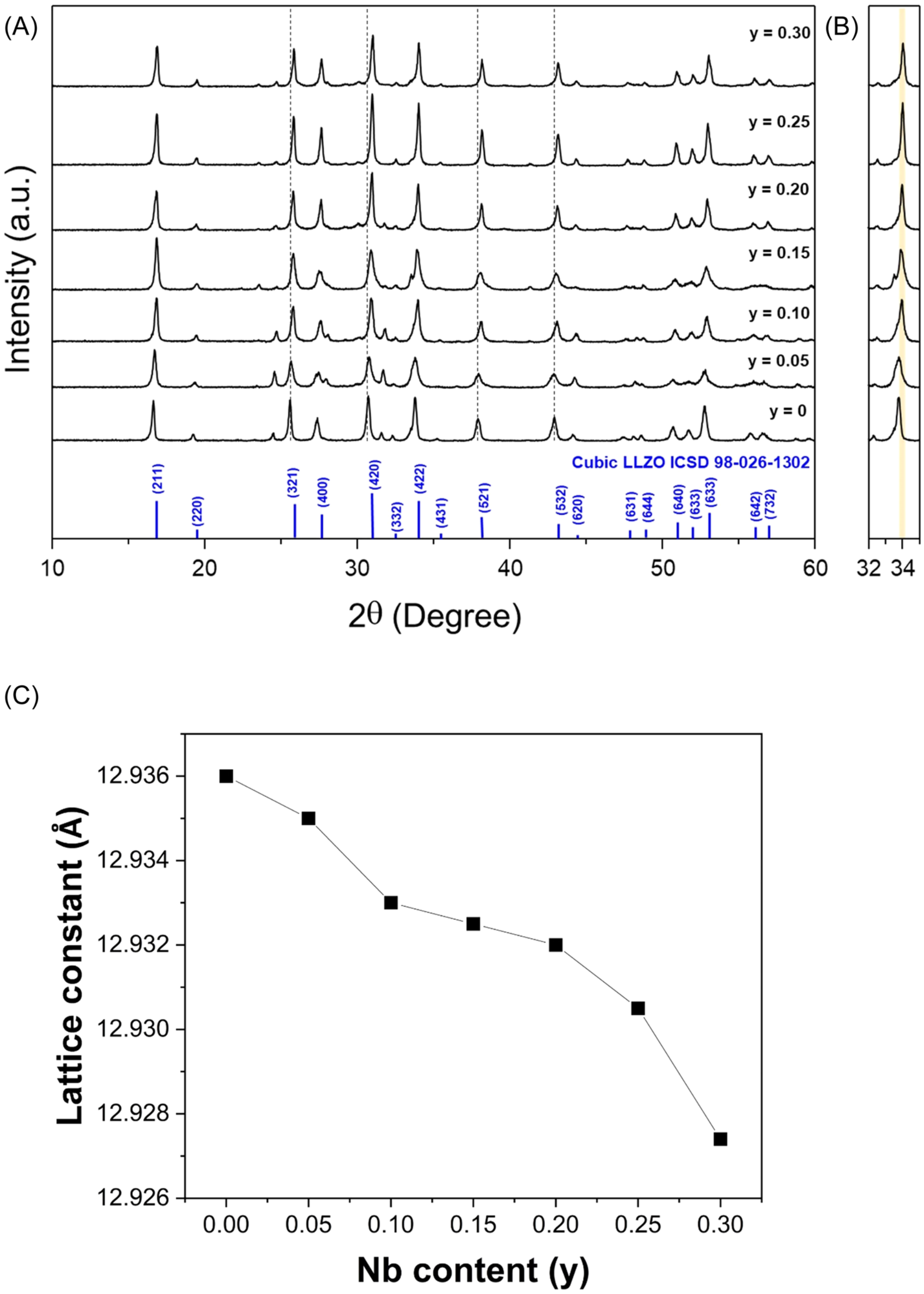

FIGURE 2 (A) XRD patterns of $Li_{6.25-y}Al_{0.25}La_3Zr_{2-y}Nb_yO_{12}$ ($0 \le y \le 0.30$), (B) enlarged XRD patterns from 32 to 34.5°, and (C) the calculated lattice constants at different stoichiometric ratios of Nb. XRD, X-ray diffraction.

LLZO after the sintering step at 1200°C, as shown in Figure 1B.

Interestingly, the effect of the Al and Nb dual-doping step was synergistic in stabilizing the cubic phase and reducing the calcination temperature. As shown in Figure 1C, the cubic phase appeared at a lower calcination temperature of 900°C, which indicates that the dual-doping method facilitates easier phase transition at a lower calcination temperature. This result is consistent with previous reports that the Al doping step stabilizes the cubic structure and decreases the calcination temperature.[20,21]

Figure 2 presents the XRD patterns of $Li_{6.25}Al_{0.25}La_3Zr_{2-y}Nb_yO_{12}$ sintered at 1200°C to investigate the effects of the Al and Nb dual-doping step on the phase transition of cubic LLZO by increasing the Nb ratio. For Al-doped LLZO without Nb ($y = 0$) as a reference sample, diffraction peaks could be indexed with the cubic phase LLZO (ICSD 98-026-1302) in the space group *I*a-3d, except for some peaks that are attributed to impurities like $LaAlO_3$ and $Li_{0.5}Al_{0.5}La_2O_4$ phases.[13,22] When the Nb content was over 0.2 ($y \geq 0.2$), Al-doped LLZO transformed into a pure cubic LLZO phase in which no clear impurity peaks were observed, as shown in Figure 2A. From the results of Rietveld refinement of XRD data (see Supporting Information: Figure S1 and S2), it was found that Al and Nb dual-doped LLZO only contained 2.5% of impurities, while Al single-doped LLZO showed 16.1% of impurities. This phase transition from the tetragonal structure to the cubic structure was also found in the results of Raman analysis, as shown in the Supporting Information: Figure S3. In the case of undoped LLZO, in the tetragonal phase, multiple peaks appear in the region of 200–500 cm^{-1} due to the ordered arrangement of Li on the tetrahedral 8a site and octahedral 16f and 32 g sites.[23] The Raman spectrum of Al and Nb codoped LLZO in the cubic phase showed two broad bands in the same region (200–500 cm^{-1}) because of the disordered highly mobile Li^+ than the ordered Li^+ in the tetragonal phase.[24]

Furthermore, an additional band appeared near 750 cm^{-1} on adding Nb. This is because the band at 750 cm^{-1} corresponds to the ZrO_6 octahedron. The additional peak at 750 cm^{-1} could be attributed to stretching of the NbO_6 octahedron.[25]

All diffraction peaks of LLZO after the Al and Nb codoping step shifted to a higher angle than that of Al single-doped LLZO. As shown in Figure 2B, diffraction peak positions at 34° tend to shift to higher angles, indicating that the lattice constant continuously decreases.[6] Lattice constants of Al and Nb codoped LLZO calculated by Rietveld refinement of data showed that their lattice constants continuously decreased with an increase in the Nb content, as shown in Figure 2C.

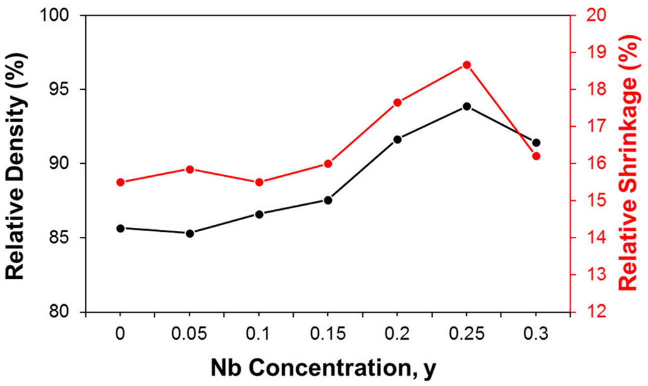

FIGURE 3 Relative densities (black) and relative shrinkage (red) of $Li_{6.25-y}Al_{0.25}La_3Zr_{2-y}Nb_yO_{12}$ ($0 \leq y \leq 0.30$) at different stoichiometric ratios of Nb

Compared to other reports, the change in the lattice constant with increasing dopant content is consistent with the relative ionic radii of Nb^{5+} (0.78 Å) and Zr^{4+} ions (0.72 Å).[6,26] The decrease of the lattice constant with an increase in the Nb content suggests a shorter mean pathway of Li ions in the 24 d and 96 h sites, allowing faster mobility of the Li ions, resulting in high ionic conductivity. The optimal range for the lattice parameter is within 12.93–12.94 Å, which is lower than previously reported values.[11]

Along with the cubic phase stabilization of LLZO, the Al and Nb codoping process affects relative densities, as shown in Figure 3. The RD and shrinkage are key factors relating to the mechanical strength and Li-ion transport properties of LLZO electrolytes. The initial relative density of 85.67% ($y = 0$) increases to a maximum of 93.87% with increasing Nb content ($y = 0.25$), and then, it decreases to 91.43% ($y = 0.3$). The low density of the LLZO pellets may have been due to impurities. The RD is consistent with the result of the RS of the samples. The RS value increased with increasing Nb ratio up to the maximum value of 18.7%, when y was 0.25, and then the values slightly decreased when y was 0.3. According to previous studies focused on hetero-atom-doped LLZO, the optimal amount of dopant promotes the densification of LLZO structures.[9,27]

Furthermore, the enhanced RD improved the ionic conductivity, which is similar to other studies.[28] Li-ion conductivities were measured by electrochemical impedance spectroscopy (EIS) of $Li_{6.25}Al_{0.25}La_3Zr_{2-y}Nb_yO_{12}$ ($y = 0.25$) at various temperature ranges under room conditions to 80°C, as shown in Figure 4. Each plot shows a rough semicircle at the high frequency and a dispersive line at the low frequency, representing the total resistance as the bulk resistance. The dispersive line suggests electrolyte–electrode polarization at the Au blocking electrodes. The high-frequency semicircle

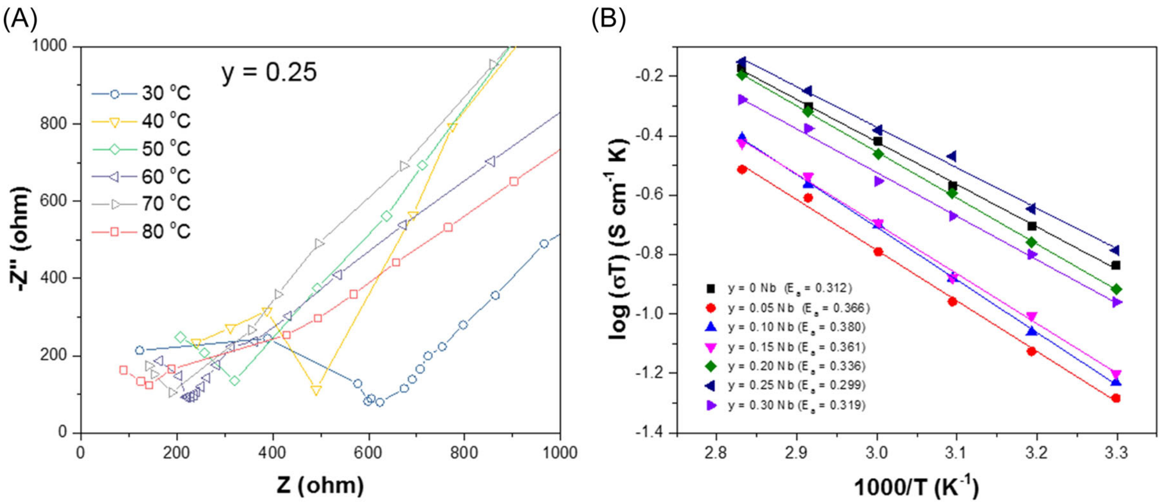

FIGURE 4 (A) Nyquist plots of sintered $Li_{6.25-y}Al_{0.25}La_3Zr_{2-y}Nb_yO_{12}$ ($y = 0.25$) with a Au blocking electrode and (B) Arrhenius plots of the total conductivity of the pellets in different temperature ranges (30–80°C)

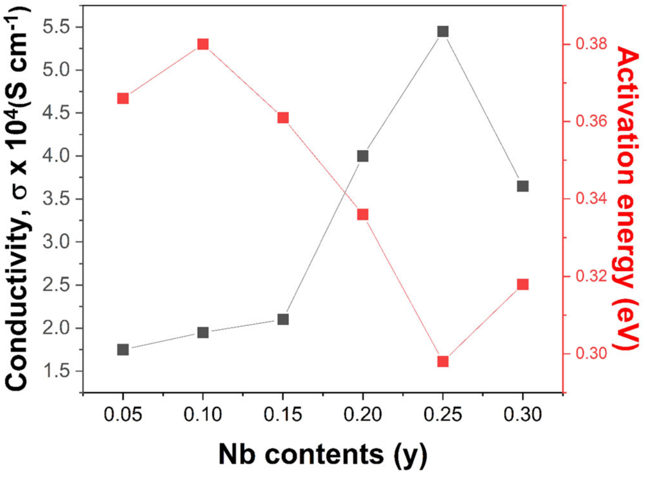

FIGURE 5 Effect of Nb contents of $Li_{6.25-y}Al_{0.25}La_3Zr_{2-y}Nb_yO_{12}$ ($0 \le y \le 0.3$) on the ionic conductivity and activation energy at 30°C

decreased and vanished with increasing temperature due to the decrease in the characteristic time and increasing Li^+ mobility, and the characteristic time exceeded the frequency window of the experiment at higher temperatures.[11] The temperature-dependent ionic conductivities of $Li_{6.25}Al_{0.25}La_3Zr_{2-y}Nb_yO_{12}$ ($y = 0.25$) LLZO are shown in Figure 4B. The ionic conductivities were best fitted with the linearized model of the Arrhenius equation as follows:

$$\sigma T = \sigma_0 \exp\left(-\frac{E_a}{k_B T}\right), \tag{3}$$

where σ is the measured ionic conductivity, σ_0 is the pre-exponential factor, E_a is the activation energy, k_B is the Boltzmann constant, and T is the absolute temperature. The high degree of linearity indicates the thermal-activated nature of lithium conductivity. Figure 5 shows the dependence of the total ionic conductivity at 30°C and its activation energy of $Li_{6.25}Al_{0.25}La_3Zr_{2-y}Nb_yO_{12}$ ($0 \le y \le 0.30$). The ionic conductivity drastically decreased to $1.75 \times 10^{-4}\ S\ cm^{-1}$ ($y = 0.05$), caused mainly by nonconducting impurity phases, as shown in the XRD pattern and low RD. The ionic conductivity gradually increased at $y > 0.10$ and reached a maximum value of $5.45 \times 10^{-4}\ S\ cm^{-1}$ at 30°C when y was 0.25. It then began to decrease to $3.62 \times 10^{-4}\ S\ cm^{-1}$ ($y = 0.30$). The indirect relation between the ionic conductivity and the activation energy suggests that an optimal stoichiometric ratio of Nb is 0.25, which can substitute the Zr sites, which yield the highest ionic conductivity at 30°C and the lowest activation energy. Since the additional Nb doping step changed Al sites from the 24d to 96 h of Li sites, the enhanced ionic conductivity may be originated.[19] These electrochemical Li-ion transport properties are consistently supported by the stabilized cubic phase with a lower level of impurities, optimal lattice constant, and a high degree of densification of the Al and Nb dual-doped LLZO electrolyte.

4 | CONCLUSION

In summary, we have demonstrated the use of the modified sol–gel synthetic method for the preparation of Al and Nb dual-doped $Li_{6.25-y}Al_{0.25}La_3Zr_{2-y}Nb_yO_{12}$ with various contents of Nb. The dual doping of Al and Nb makes the cubic phase more stable at a calcination temperature lower than 900°C. Moreover, the Al and Nb dual-doping strategy enhances the degree of solidification for cubic phase LLZO with the addition of Nb, which leads to an improvement of Li-ion conductivity to 5.45×10^{-4} S cm^{-1} at 30°C. Based on these results, we found that $Li_6Al_{0.25}Zr_{1.75}Nb_{0.25}O_{12}$ is the optimal composition in terms of LLZO densification, lattice constant, and electrochemical ionic conductivity.

ACKNOWLEDGMENTS

This research was supported by the National R&D Program through the National Research Foundation of Korea (NRF) funded by the Ministry of Science and ICT (NRF-2021K1A48A01079455).

CONFLICT OF INTEREST

The authors declare no conflict of interest.

DATA AVAILABILITY STATEMENT

The data that support the findings of this study are available from the corresponding author upon reasonable request.

ORCID

Jaeyoung Lee http://orcid.org/0000-0002-9392-5576

REFERENCES

1. Bachman JC, Muy S, Grimaud A, et al. Inorganic solid-state electrolytes for lithium batteries: mechanisms and properties governing ion conduction. *Chem Rev*. 2016;116(1):140-162.
2. Takada K. Progress and prospective of solid-state lithium batteries. *Acta Mater*. 2013;61(3):759-770.
3. Kokal I, Somer M, Notten PHL, Hintzen HT. Sol-gel synthesis and lithium ion conductivity of $Li_7La_3Zr_2O_{12}$ with garnet-related type structure. *Solid State Ion*. 2011;185(1):42-46.
4. Murugan R, Thangadurai V, Weppner W. Fast lithium ion conduction in garnet-type $Li_7La_3Zr_2O_{12}$. *Angew Chemie Int Ed*. 2007;46(41):7778-7781.
5. Yu S, Schmidt RD, Garcia-Mendez R, et al. Elastic properties of the solid electrolyte $Li_7La_3Zr_2O_{12}$ (LLZO). *Chem Mater*. 2016;28(1):197-206.
6. Yang T, Li Y, Wu W, et al. The synergistic effect of dual substitution of Al and Sb on structure and ionic conductivity of $Li_7La_3Zr_2O_{12}$ ceramic. *Ceram Int*. 2018;44(2):1538-1544.
7. Miara LJ, Richards WD, Wang YE, Ceder G. First-principles studies on cation dopants and electrolyte/cathode interphases for lithium garnets. *Chem Mater*. 2015;27(11):4040-4047.
8. Song S, Sheptyakov D, Korsunsky AM, Duong HM, Lu L. High Li ion conductivity in a garnet-type solid electrolyte via unusual site occupation of the doping Ca ions. *Mater Des*. 2016;93:232-237.
9. Allen JL, Wolfenstine J, Rangasamy E, Sakamoto J. Effect of substitution (Ta, Al, Ga) on the conductivity of $Li_7La_3Zr_2O_{12}$. *J Power Sources*. 2012;206:315-319.
10. Kumazaki S, Iriyama Y, Kim KH, et al. High lithium ion conductive $Li_7La_3Zr_2O_{12}$ by inclusion of both Al and Si. *Electrochem Commun*. 2011;13(5):509-512.
11. Wang D, Zhong G, Dolotko O, et al. The synergistic effects of Al and Te on the structure and Li^+-mobility of garnet-type solid electrolytes. *J Mater Chem A*. 2014;2(47):20271-20279.
12. Rettenwander D, Redhammer G, Preishuber-Pflügl F, et al. Structural and electrochemical consequences of Al and Ga cosubstitution in $Li_7La_3Zr_2O_{12}$ solid electrolytes. *Chem Mater*. 2016;28(7):2384-2392.
13. Ohta S, Kobayashi T, Asaoka T. High lithium ionic conductivity in the garnet-type oxide $Li_{7-X}La_3(Zr_{2-X}, Nb_X)O_{12}$ ($X = 0$-2). *J Power Sources*. 2011;196(6):3342-3345.
14. Paulus A, Kammler S, Heuer S, et al. Sol gel vs solid state synthesis of the fast lithium-ion conducting solid state electrolyte $Li_7La_3Zr_2O_{12}$ substituted with iron. *J Electrochem Soc*. 2019;166(3):A5403-A5409.
15. Banik A, Famprikis T, Ghidiu M, Ohno S, Kraft MA, Zeier WG. On the underestimated influence of synthetic conditions in solid ionic conductors. *Chem Sci*. 2021;12(18):6238-6263.
16. Janani N, Ramakumar S, Dhivya L, Deviannapoorani C, Saranya K, Murugan R. Synthesis of cubic $Li_7La_3Zr_2O_{12}$ by modified sol-gel process. *Ionics (Kiel)*. 2011;17(7):575-580.
17. Im C, Park D, Kim H, Lee J. Al-incorporation into $Li_7La_3Zr_2O_{12}$ solid electrolyte keeping stabilized cubic phase for all-solid-state Li batteries. *J Energy Chem*. 2018;27(5):1501-1508.
18. Yang SH, Kim MY, Kim DH, et al. Ionic conductivity of Ga-doped LLZO prepared using Couette–Taylor reactor for all-solid lithium batteries. *J Ind Eng Chem*. 2017;56:422-427.
19. Shin DO, Oh K, Kim KM, et al. Synergistic multi-doping effects on the $Li_7La_3Zr_2O_{12}$ solid electrolyte for fast lithium ion conduction. *Sci Rep*. 2015;5:1-9.
20. Chen RJ, Huang M, Huang WZ, Shen Y, Lin YH, Nan CW. Effect of calcining and Al doping on structure and conductivity of $Li_7La_3Zr_2O_{12}$. *Solid State Ion*. 2014;265:7-12.
21. El-Shinawi H, Paterson GW, MacLaren DA, Cussen EJ, Corr SA. Low-temperature densification of Al-doped $Li_7La_3Zr_2O_{12}$: a reliable and controllable synthesis of fast-ion conducting garnets. *J Mater Chem A*. 2017;5(1):319-329.
22. Rangasamy E, Wolfenstine J, Sakamoto J. The role of Al and Li concentration on the formation of cubic garnet solid electrolyte of nominal composition $Li_7La_3Zr_2O_{12}$. *Solid State Ion*. 2012;206:28-32.
23. Dhivya L, Karthik K, Ramakumar S, Murugan R. Facile synthesis of high lithium ion conductive cubic phase lithium garnets for electrochemical energy storage devices. *RSC Adv*. 2015;5(116):96042-96051.
24. Dhivya L, Murugan R. Effect of simultaneous substitution of y and Ta on the stabilization of cubic phase, microstructure, and Li^+ conductivity of $Li_7La_3Zr_2O_{12}$ lithium garnet. *ACS Appl Mater Interfaces*. 2014;6(20):17606-17615.

25. Thompson T, Wolfenstine J, Allen JL, et al. Tetragonal vs. cubic phase stability in Al-free Ta doped $Li_7La_3Zr_2O_{12}$ (LLZO). *J Mater Chem A*. 2014;2:13431-13436.
26. Shannon BYRD HM, Baur NH, Gibbs OH, Eu M, Cu V. Revised effective ionic radii and systematic studies of interatomie distances in halides and chaleogenides. *Acta Crystallogr A*. 1976;32(5):751-767.
27. Wolfenstine J, Rangasamy E, Allen JL, Sakamoto J. High conductivity of dense tetragonal $Li_7La_3Zr_2O_{12}$. *J Power Sources*. 2012;208:193-196.
28. Gupta A, Murugan R, Paranthaman MP, et al. Optimum lithium-ion conductivity in cubic $Li_{7-x}La_3Hf_{2-x}Ta_xO_{12}$. *J Power Sources*. 2012;209:184-188.

SUPPORTING INFORMATION

Additional supporting information can be found online in the Supporting Information section at the end of this article.

How to cite this article: Kim JW, Digol JL, Bong S, Lee J. Enhanced Li-ion conductivity of $Li_7La_3Zr_2O_{12}$ by simultaneous substitution of aluminum and niobium using a modified sol–gel method. *Battery Energy*. 2023;2:20220024. doi:10.1002/bte2.20220024